Contents

1 Two alternative models

Two diffrent general models can be used to describe efficient Cdc20 inhibition in the context of an emitted signal. Broadly speaking Cdc20 can be inhibited either by *sequestering* or by *degradation* (supplementory fig. 1). In the sequestering case it is assumed that Cdc20 "c" is tethered by the an emitted active complex "m^*". This tethering can be either direct, through physical binding or indirect by phosphorylation. In the degradation case it's simply assumed that the inhibition is achieved though a checkpoint mediated upregulation of the degradation rate (by the active emitted complex). Modeling the two cases with systems if ordinary differential equations we get:

For the degradation case:

$$\frac{dm}{dt} = k_m m^* - k_{-m} m + k^{on}_{deg.} m^* c \tag{1}$$

$$\frac{dm^*}{dt} = -k_m m^* + k_{-m} m - k^{on}_{deg.} m^* c \tag{2}$$

$$\frac{dc}{dt} = k_{prod.} - k^{on}_{deg.} m^* c - k^{off}_{deg} c \tag{3}$$

$$m_{tot} = m + m^* \tag{4}$$

and for the sequestering case:

$$\frac{dm}{dt} = k_m m^* - k_{-m} m + (k_{deg.} + k_{diss.}) m^c \tag{5}$$

$$\frac{dm^*}{dt} = -k_m m^* + k_{-m} m - k_{ass.} m^* c \tag{6}$$

$$\frac{dc}{dt} = k_{prod.} - k_{ass.} m^* c - k_{deg.} c + k_{diss.} m^c \tag{7}$$

$$\frac{dm^c}{dt} = -(k_{deg.} + k_{diss.}) m^c + k_{ass.} m^* c \tag{8}$$

$$m_{tot} = m + m^* + m^c \tag{9}$$

2 Simplifications and Assumptions

Several assumptions and simplifications were made in order to simplify the analysis of the models.

2.1 m_{tot} constant

We assumed that the total amount of m is constant. The reason for this is that the mRNA levels of Mad1, Mad2, Mad3, Bub1 and Bub3 are more or less constant during the cell cycle (with the possible exeption of Bub1) [1].

2.2 m, m^* equilibriate fast

This assumption implicates that the active checkpoint depends on the rates $k_{ass.}$ and $k_{deg.}^{on}$ rather then k_{-m}. There are two reasons for this assumption: First it's biologically motivated since both the turnover of checkpoint proteins at the kinetochore [5] and the overall reaction dynamics of the checkpoint is very fast (the checkpoint has to control the amount of emitted complexes one way or another rapidly). Second, it simplifies the analytical treatment of the systems without changing the overall results (see suppl. figures 4, 5, 6 and 10 where we verify the analytically obtained solutions against the unsimplified systems).

2.3 m^* converts to m after deinhibition/degradation

By assuming that m^* is converted to m after deinhibition/degradation we allow the checkpoint to control the reaction in the simplest possible manner. The alternative, to add a extra "deactivation/dephosphorylation rate" which controls the $m^* \rightarrow m$ reaction would not only complicate the model, it also fails to show any different quantitative result (unpublished results).

2.4 Efficient inhibition is achieved

We also assume that both models are capable of inhibiting Cdc20. That is, we assume that the models are capable of lowering the amount of Cdc20 enough times to ensure good inhibition (see below for all details). The exact nature of the inhibition depends on the model, either the degradation or phosphorylation rates are high enough, or we have an excess of m complex in the system.

2.5 Lengthscale

What effect does the spatiality have on the system? The general idea was that if we have a continous influx of Cdc20 from the boundary it might be harder for the checkpoint to degrade it properly. To test this, we used FEMLAB to simulate the effects of Cdc20 influx into the nucleus. The nucleus was modeled as a sphere and the influx was either from the entire boundary or from one

to several pointlike sources symmetrically located on it. The approximate area covered by the intervall of point sources was varied from a single point source through the approximate area covered by the nuclear pores [2] to a complete covering of the boundary. We found that for realistic parameters the spatial effects were not very pronounced and therefore decided to use ODEs (suppl. Fig 2).

3 System characteristics

Three different measures were extracted from these systems of ODEs, the *amplification*, the *reactivation time* and the *noise resistance*.

3.1 Amplification

We define the amplification "ρ", as the steady state level of uninhibited c when the checkpoint is off ($k_{-m} = 0$), divided by the steady state level of uninhibited c when the checkpoint is on, that is:

$$\rho = \frac{c^{off}_{st.st.}}{c^{on}_{st.st.}} \tag{10}$$

This gave us the following amplification for the two models:

Degradation model

The steady state solutions for the cases were the checkpoint is "on" or "off" was found to be:

$$c^{off}_{st.st.} = \frac{k_{prod.}}{k^{off}_{deg.}}, \quad c^{on}_{st.st.} = \frac{k_{prod.}}{k_c + k^{off}_{deg.}}, \quad \Rightarrow \rho_{deg.} = \frac{k_c}{k_{deg.}} + 1 \tag{11}$$

If we assume that the system is capable of inhibiting the Cdc20 in an efficient way then $\rho >> 1$, which means that we can approximate ρ to:

$$\rho = \frac{k_c}{k_{deg.}} \tag{12}$$

This expression was verified vs. the exact numerical solution (suppl. fig.4(a)).

Sequestering model

The solution for the "off"-case in steady state is easily obtained:

$$c^{off}_{st.st.} = \frac{k_{prod.}}{k_{deg.}} \tag{13}$$

In the "on" case we have the following equations in steady state:

$$0 = k_{prod.} - k_c c - k_{deg.} c + k_{diss.} m^c \tag{14}$$
$$0 = -(k_{deg.} + k_{diss.}) m^c + k_c c \tag{15}$$

We eliminate m^c and get the following expression:

$$0 = k_{prod.} - c^{on}_{st.st.} \left(k_c + k_{deg.} - \frac{k_{diss.} k_c}{k_{deg.} + k_{diss.}} \right) \Leftrightarrow c^{on}_{st.st.} = \frac{k_{prod.}}{k_c + k_{deg.} - \frac{k_{diss.} k_c}{k_{diss.} + k_{deg}}} \tag{16}$$

This expression is further simplified to:

$$c^{on}_{st.st.} = \frac{k_{prod.}}{k_{deg.}} \frac{k_{deg.} + k_{diss.}}{k_c + k_{deg.} + k_{diss.}} \tag{17}$$

Which gives the following ρ:

$$\rho = \frac{k_c + k_{deg.} - \frac{k_{diss.} k_c}{k_{diss.} + k_{deg}}}{k_{deg.}} = ... = \frac{k_c}{k_{deg.} + k_{diss.}} + 1 \cong \frac{k_c}{k_{deg.} + k_{diss.}} \tag{18}$$

Again we assumed that the inhibition is effective, ie $\rho >> 1$. This expression was also verified against its numeric counterpart (suppl. fig. 4(b)).

3.2 Noise resistance

We investigated the models resistence to noise in the Cdc20 production. There are mainly two reasons why we only look at noise in the Cdc20 and not also in the inhibitory signal: First the copy numbers of the constituents of the MCC complex is more or less constant during the cell-cycle (see section 2.1) and in relative abundance 5. Second, Cdc20 is the crucial component in the system and can therefore not be allowed to be active at any time until the checkpoint ceases to work (see the main text). Unless the copynumber of the inhibitory signal drops drastically, noise in it will have no or little effect. This is contrasted by the fact that Cdc20 needs to be kept down all the time.

In order to quantisize the model's response to noise we defined an expression for the models noise resistance as a function of the length of the perturbation $\xi(t)$. What we want to measure is how robust the system is to a perturbation in the Cdc20 production rate. Since any model will yield to a change in the production rate if it's long enough, we decided to investigate the dynamics of such a response, or the time it takes to reach a new (perturbed) steady state as a function of the model parameters after exposure to an increase in the Cdc20 production rate of time t.

I.e. we are looking at the system in an initial steady state, c_{low} or $c(t = 0)$, when it suddenly is exposed to an everlasting arbitrary high increase in the

Cdc20 production rate $k_{prod.}$. After this, the increase of c as a function of time is measured as it goes towards its new steady-state c_{high} or $c(t = \infty)$. Subsequently, the function of $c(t)$ is normalized with the difference between the two steady states so that we get an estimate of the noise resistence between one and zero. For aestetic reasons one is deducted from this value from this value so that values towards "1" means very good noise resistance and towards "0" means very poor noise resistance, that is:

$$\xi(t) = 1 - \frac{c(t) - c_{low}}{c_{high} - c_{low}} \tag{19}$$

Please see also supplementory figure 3 for a graphic interpretation.

Degradation model

If we perturb the production rate of c, $k_{prod.}$, for long enough time, its level changes from c_{low} to c_{high}. For simplicity it was assumed that $k_{prod.}^{perturbed} > k_{prod}^{"normal''}$. Using our assumption from section 2.2, that m and m^* are in a fast equilibrium we can solve eq. 3 to get $c(t)$:

$$c(t) = c_{high} - (c_{high} - c_{low}) exp^{-(k_{deg.} + k_c)t} \tag{20}$$

This gives the following noise resistance:

$$\begin{aligned} &\xi(t) = 1 - \frac{c(t) - c_{low}}{c_{high} - c_{low}} = 1 - \frac{c_{high} - (c_{high} - c_{low}) e^{-(k_{deg.} + k_c)t} - c_{low}}{c_{high} - c_{low}} \\ &\Rightarrow \xi(t) \cong e^{-k_c t} \end{aligned} \tag{21}$$

Again we used that $\rho >> 1$ which means that $k_c >> k_{deg.}$ (from eq. 12). This analytical expression was verified against the numerical one (suppl. fig. 5(a)).

Sequestering model

In order obtain $c(t)$, equation 7 and 8 were rewritten:

$$\frac{d}{dt} \begin{pmatrix} m^c \\ c \end{pmatrix} = \begin{pmatrix} -(k_{deg.} + k_{diss.}) & k_c \\ k_{diss.} & -(k_{deg.} + k_c) \end{pmatrix} \begin{pmatrix} m^c \\ c \end{pmatrix} + \begin{pmatrix} 0 \\ k_{prod.} \end{pmatrix} \tag{22}$$

As in the previous section it was assumed that m and m^* are in fast equlibrium (sec. 2.2). Next the eigenvalues were determined:

$$\lambda_1 = -k_{deg.} \tag{23}$$

$$\lambda_2 = -(k_{deg.} + k_{diss.} + k_c) \tag{24}$$

Which gives the following eigenvectors:

$$v_1 = \begin{pmatrix} k_c/k_{diss.} \\ 1 \end{pmatrix} \tag{25}$$

$$v_2 = \begin{pmatrix} -1 \\ 1 \end{pmatrix} \tag{26}$$

We thus have the general solution c_g for the homogenous system:

$$c_g(t) = C_1 \begin{pmatrix} k_c/k_{diss.} \\ 1 \end{pmatrix} e^{-k_{deg.}t} + C_2 \begin{pmatrix} -1 \\ 1 \end{pmatrix} e^{-(k_{deg.}+k_{diss.}+k_c)t} \tag{27}$$

We now looked for the particular solution c_p, due to the time-independence of the constant term, we simply assumed a constant particular solution $\bar{z}$:

$$\bar{z} = \begin{pmatrix} z_1 \\ z_2 \end{pmatrix} \Rightarrow \begin{pmatrix} 0 \\ 0 \end{pmatrix} = \begin{pmatrix} -(k_{deg.}+k_{diss.}) & k_c \\ k_{diss.} & -(k_{deg.}+k_c) \end{pmatrix} \begin{pmatrix} z_1 \\ z_2 \end{pmatrix} + \begin{pmatrix} 0 \\ k_{prod.} \end{pmatrix} \tag{28}$$

Solving for $\bar{z}$ gives:

$$\begin{pmatrix} z_1 \\ z_2 \end{pmatrix} = \frac{k_{prod.}}{k_{deg.}} \begin{pmatrix} \frac{k_c}{k_c+k_{diss.}+k_{deg.}} \\ \frac{k_{diss.}+k_{deg.}}{k_c+k_{diss.}+k_{deg.}} \end{pmatrix} \tag{29}$$

Obviously z_1 and z_2 corresponds to the steady-state levels of c and m^c, that is:

$$\begin{pmatrix} z_1 \\ z_2 \end{pmatrix} = \begin{pmatrix} m^c_{st.st.} \\ c_{st.st.} \end{pmatrix} \tag{30}$$

Moreover we note that the ratio between the two equals the amplification:

$$\frac{z_1}{z_2} = \frac{k_c}{k_{deg.}+k_{diss.}} = \rho \tag{31}$$

so that we can write:

$$\bar{z} = \begin{pmatrix} \rho c_{st.st.} \\ c_{st.st.} \end{pmatrix} \tag{32}$$

Equation 22 thus have the following general solution:

$$\begin{pmatrix} m^c(t) \\ c(t) \end{pmatrix} = C_1 \begin{pmatrix} k_c/k_{diss.} \\ 1 \end{pmatrix} e^{-k_{deg.}t} + C_2 \begin{pmatrix} -1 \\ 1 \end{pmatrix} e^{-(k_{deg.}+k_{diss.}+k_c)t} + \begin{pmatrix} \rho c_{st.st.} \\ c_{st.st.} \end{pmatrix} \tag{33}$$

We can now use the following boundary conditions to find C_1 and C_2: Assume that we are in a steady state with a certain production rate of c at time zero, "$k^0_{prod.}$" corresponding to "c_{low}", and then increase it to "$k^{incr.}_{prod.}$" so that we arrive at a new steady state "c_{high}" after an arbitrary long time we get that:

$$\begin{pmatrix} \rho c_{low} \\ c_{low} \end{pmatrix} = C_1 \begin{pmatrix} k_c/k_{diss.} \\ 1 \end{pmatrix} + C_2 \begin{pmatrix} -1 \\ 1 \end{pmatrix} + \begin{pmatrix} \rho c_{high} \\ c_{high} \end{pmatrix} \tag{34}$$

$c_{high} - c_{low}$ is now denoted "Δc", which gives the following equation:

$$-\begin{pmatrix} \rho \Delta c \\ \Delta c \end{pmatrix} = C_1 \begin{pmatrix} k_c/k_{diss.} \\ 1 \end{pmatrix} + C_2 \begin{pmatrix} -1 \\ 1 \end{pmatrix} \tag{35}$$

Solving for C_1 and C_2 now gives:

$$C_1 = -\Delta c \left(\frac{k_{diss.}}{k_{diss.} + k_{deg.}} \frac{k_{diss.} + k_{deg.} + k_c}{k_{diss.} + k_{k_c}} \right) \quad C_2 = -\Delta c \left(\frac{k_c}{k_{diss.} + k_c} \frac{k_{deg.}}{k_{deg.} + k_{diss.}} \right) \tag{36}$$

Both these formulae can be simplified somewhat due to the fact that $\rho >> 1 \Rightarrow k_c >> k_{diss.} \& k_{deg.}$ (eq 18):

$$C_1 \cong -\Delta c \frac{k_{diss.}}{k_{diss.} + k_{deg.}} \quad C_2 \cong -\Delta c \frac{k_{deg.}}{k_{deg.} + k_{diss.}} \tag{37}$$

We can now find $c(t)$ from eq.s 33 and 37 and calculate the noise resistance as defined by eq. 19:

$$\xi(t) = 1 - \Delta c \left(-\frac{k_{diss.}}{k_{diss.} + k_{deg.}} e^{-k_{deg.} t} - \frac{k_{deg.}}{k_{deg.} + k_{diss.}} e^{-(k_c + k_{diss.} + k_{deg.})t} + 1 \right) / \Delta c \tag{38}$$

This expression can also be simplified, if $\rho >> 1$ we can neglect the second exponential term and get the expression for the noise resistance in its final form:

$$\xi(t) = \frac{k_{diss.}}{k_{diss.} + k_{deg.}} e^{-k_{deg.} t} \tag{39}$$

Also this analytical approximation of the noise resistance was consistent with its numerical counterpart (suppl. fig. 5(b)).

3.3 Reactivation

We defined the reactivation time "τ" as the time it takes to reach 90% of the $c^{off}_{st.st.}$ after the checkpoint shutdown. Since m and m^* are in fast equilibrium (sec. 2.2) the checkpoint only depends on the k_c rate so by setting it to zero (checkpoint deactivation) we can solve $c(t)$ in the two cases:

Degradation model

When $k_c = 0$, we can solve eq. 3 which gives a $c(t)$ of the following form:

$$c(t) = \frac{k_{prod.}}{k_{deg.}^{off}} - \left(\frac{k_{prod.}}{k_{deg.}^{off}} - \frac{k_{prod.}}{k_{deg.}^{off} + k_c} \right) e^{-k_{deg.}^{off} t} \tag{40}$$

This means that the time it takes to reach 90% of the "off" steady-state, τ is:

$$\tau = -\frac{1}{k_{deg.}} ln \left(\frac{0.1 k_{prod.}/k_{deg.}}{\frac{k_{prod.}}{k_{deg.}} - \frac{k_{prod.}}{k_{deg.}+k_c}} \right) = \frac{1}{k_{deg.}} ln \left(\frac{10}{1 - \frac{1}{1+\frac{k_c}{k_{deg.}}}} \right) \backsimeq \frac{1}{k_{deg.}} ln(10) \tag{41}$$

This expression was verified with its numerical solution in suppl. fig. 6(a).

Sequestering model

When $k_c = 0$ (checkpoint deactivation) we got the following equation for m^c:

$$\frac{dm^c}{dt} = -m^c(k_{deg.} + k_{diss.}) \Rightarrow m(t)^c = m_{st.st.}^c e^{-(k_{deg.}+k_{diss.})t} \tag{42}$$

Since $m_{st.st.}^c$ is already known from eq:29 and 30, equation 7 can be rewritten as:

$$\frac{dc}{dt} = k_{prod.} - k_{deg.} c + k_{diss.} m_{st.st.}^c e^{-(k_{deg.}+k_{diss.})t} \tag{43}$$

This equation has the following general solution:

$$c(t) = \frac{k_{prod.}}{k_{deg.}} + C e^{-k_{deg.} t} - m_{st.st.}^c e^{-(k_{deg.}+k_{diss.})t} \tag{44}$$

Here C is a constant to be determined from the initial and final steady states of the system that is:

$$c(t=0) = c_{st.st.}^{on} \quad \text{and} \quad c(t=\infty) = c_{st.st.}^{off} \tag{45}$$

Where $c_{st.st.}^{off}$ and $c_{st.st.}^{on}$ are known from eqs:13 and 17. Using the initial condition for $t = 0$ we get that:

$$c_{st.st.}^{on} = \frac{k_{prod.}}{k_{deg.}} \frac{k_{deg.} + k_{diss.}}{k_c + k_{diss.} + k_c} = C - \frac{k_{prod.}}{k_{deg.}} \frac{k_c}{k_c + k_{diss.} + k_{deg.}} + \frac{k_{prod.}}{k_{deg.}} \tag{46}$$

We used eq. 32 for the value of $m_{st.st.}^c$. Solving this equation we see that $C = 0$, which gives us the final form of $c(t)$:

$$c(t) = \frac{k_{prod.}}{k_{deg.}} \left(1 - \frac{k_c}{k_c + k_{diss.} + k_{deg.}} e^{-(k_{diss.}+k_{deg.})t} \right) \tag{47}$$

In order to determine the time it takes to reach a certain fraction "x" of the final level ($c^{off}_{st.st.} = k_{prod.}/k_{deg.}$), we solve the following equation for the reactivation time τ:

$$x\frac{k_{prod.}}{k_{deg.}} = \frac{k_{prod.}}{k_{deg.}}\left(1 - \frac{k_c}{k_c + k_{diss.} + k_{deg.}}e^{-(k_{diss.}+k_{deg.})\tau}\right) \tag{48}$$

we get that:

$$(1-x)\frac{k_c + k_{diss.} + k_{deg.}}{k_c} = e^{-(k_{diss.}+k_{deg.})\tau} \tag{49}$$

which is the same as:

$$(1-x)(1+1/\rho) = e^{-(k_{diss.}+k_{deg.})\tau} \Rightarrow (1-x) \cong e^{-(k_{diss.}+k_{deg.})\tau} \tag{50}$$

Again we used that $\rho >> 1$, we now get the final form for the reactivation time τ:

$$\tau = \frac{ln(1-x)}{-(k_{diss.} + k_{deg.})} \quad \text{for } x = 0.9 \text{ we get that:} \quad \tau = \frac{ln(10)}{k_{diss.} + k_{deg.}} \tag{51}$$

Also this expression was verified vs. its numerical solution (suppl. fig. 6(b)).

4 Limitations

By restraining ρ, τ, and $\xi(t)$, we were able to investigate their interplay.

4.1 Degradation model

We defined the noise resistance as adequately good if $\xi < e^{-1}$. This gives that $1/t > k_c$ (eq:21). We furthermore demand that $k_c/k_{deg.} > \rho$ for some ρ (eq.11) and that $\tau < ln(10)/k_{deg.}$ for some τ (eq:41). In conclusion we get:

$$\frac{1}{t} > k_c > \rho k_{deg.} > \frac{\rho ln(10)}{\tau} > \frac{\rho}{\tau} \Rightarrow t < \frac{\tau}{\rho} \tag{52}$$

This means that the maximal length of a tolerated perturbation is smaller than the reactivation time divided by the amplification.

4.2 Sequestering model

Given the equations for the amplification, noise sensitivity and reactivation (eq:s 18, 29 and 51) we estimate how a maximal tolerated pulse length depends on the parameters and constraints. We have that:

$$\frac{ln(10)}{\tau_{critical}} < k_{deg.} + k_{diss.} < \frac{k_c}{\rho_{minimal}} \qquad \text{and} \qquad \xi(t_{limit}) = \frac{k_{diss.}}{k_{deg.} + k_{diss.}} e^{-k_{deg.} t_{limit}} \tag{53}$$

In order to have good noise resistance, i.e. $\xi > e^{-1}$ we need to fulfill two conditions:

$$\begin{aligned} (1): &\quad k_{deg.} < 1/t_{limit} \\ (2): &\quad k_{diss.} > k_{deg.} \end{aligned} \tag{54}$$

From these conditions it becomes clear that the limits imposed on $k_{deg.}$ and $k_{diss.}$ in eq:53 doesn't restrict the noise resistance. According to these constraints $k_{deg.}$ don't have a lower limit (first condition) and we are only interested in the relation between $k_{deg.}$ and $k_{diss.}$, not in their absolute values (second condition). Obviously for biological reasons $k_{deg.}$ cannot approach zero but the fact that it's not constrained by the mechanisms of this model still holds.

4.3 A combination of the two models

What happens if we combine the two models? That is, if we allow the degradation rate from m^c to be higher than $k_{deg.}$? Denoting the new enhanced degradation rate as "k_3" we get that the new steady state for c^{on}:

$$c^{on}_{st.st.} \frac{k_{prod.}}{k_{deg.} + k_c \frac{k_3}{k_3 + k_{diss.}}} \tag{55}$$

Here we have two cases: If $k_3 < k_{diss.}$ then the inhibition will scale linearly with k_3 else if $k_3 > k_{diss.}$ only $k_c/k_{diss.}$ will effect the inhibition (and we are effectively back in the degradation model). That the inhibition (or amplification, which is linear with the inhibition since the "off"-state is constant) is indeed proportional to this expression is verified in suppl. figure 7.

Where the inhibition increases with the rate k_3 the noise resistance decreases, since we move more and more towards the degradation case (suppl. fig.8).

5 A comparison between the deterministic and the stochastic formulations

We also compared the deterministic estimates of ρ,τ and ξ with stochatic simulations of the models. This was done using the Gillespie algoritm [3]. The total amount of m was set to 1000, a value lower but in the same magnitude as the estimated copynumbers of the Cdc20 binding proteins [4] ($\#Mad2 \sim 1.1e3$, $\#Mad3 \sim 3.17e3$, $\#Bub1 \sim 4.14e2$, $\#Bub3 \sim 1.43e3$). This value is, as stated above, not an absolute demand. It can be lowered at least a magnitude depending on the association rate/"on"-degradation rate. A typical gillespie simulation is shown in supplementary figure 9.

5.1 Amplification and reactivation

More comprehensive simulations of the models were also done. In order to get decent fits between the analytical estimates and the numeric simulations, two things were demanded: First, the system we are looking at has to be in equilibrium before we perturb it, this generally means that the simulations has too be long. Second, in order to capture rapid events such as the reactivation we need as good resolution as possible which implies that we sample often. Another intersting feature of the stochastic approach is that we can impose an additional demand on the system, regarding low copynumbers (an amplification of 100 is not very useful if it decreases the copynumber from $10e6$ to $10e4$). When tested for a broader range of parameters (see suppl. fig. 10), we see that the estimates fits quite well, it should also be noted that the less c, the lower ρ and the shorter reactivation time the worse the fit between analytical estimate and numerical simulation.

5.2 Noise resistance

We also tested the noise resistance for the two models:

Sequestering model: Due to the long time necessary for each simulation we choose to look at a smaller range of parameters (see. suppl. table1). Still as far as we see the numerical results and the analytical estimates are in good agreement for a much broader parameter range, given long and frequent enough simulations.

$k_{diss.} \rightarrow$ $k_{deg.} \downarrow$	$1.0s^{-1}$	$2.2s^{-1}$	$4.6s^{-1}$
$0.10s^{-1}$	1.010	1.014	NaN
$0.32s^{-1}$	1.071	1.062	1.057
$1.00s^{-1}$	1.116	1.070	1.101

Table 1: the ratio between the estimated and numerical noise resistance times of the sequestering model, simulation length was 200000 X 250. Three factors seem to determine the size of the error, the length of the simulation, the resolution of the simulation (how often we sample) and the estimated length of the noise resistance. Small t-values are noiser than longer ones. If we could make a longer simulation while keeping a high resolution of the events this error would decrease. The NaN value occurs when a simulations hasn't run long enough. Parameters used: $k_{prod.} = 20Ms^{-1}$, $k_m = 100s^{-1}$ and $k_{-m} = 1000s^{-1}$.

Degradation model: It proved quite hard to test the noise resistance in the degradation model, mainly due to the fact that it's so low. In practice we had to weaken the amplification and lower the total amount of emitted complexes in order to compare the analytical estimate and the numerical values in a reasonable way. Such an approach however violate the assumption that $\rho >> 1$. Practically this means that we have to fine tune the parameters in order to get a noise resistence that fits the estimate, one such example can be seen in suppl. figure 9.

6 Bode plots of the two models

In order to further compare the two models we formulated the transfer functions of the two models and plotted their responses for different frequencies in a Bode plot (suppl. fig 11). We see that indeed the sequestering model seems to buffer noise in a broader range of frequencies.

7 Supplementory references

References

[1] Spellman P.T. et. al (1998) *Molecular Biology of the cell* **9,** 3273-3297.

[2] Adam S.A. (2001) *Genome Biol.* **2(9)**

[3] Gillespie D. (1977) *J. Phys. Chem.* **81,** 2340-2362.

[4] Ghaemmaghami S. et. al (2003) *Nature* **425,** 737-41.

[5] Howell B.J. et. al (2004) *Curr. Biol.* **14,** 953-64.

8 Supplementory figures

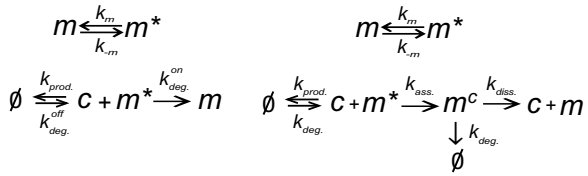

Figure 1: Two alternative models, *degradation model* (left) The degradation rate of Cdc20 is upregulated by the checkpoint. *sequestering model* (right) activated checkpoint proteins binds and sequesters Cdc20. Cdc20 is denoted "c", the inactive emitted complex "m" and the active one is "m^*".

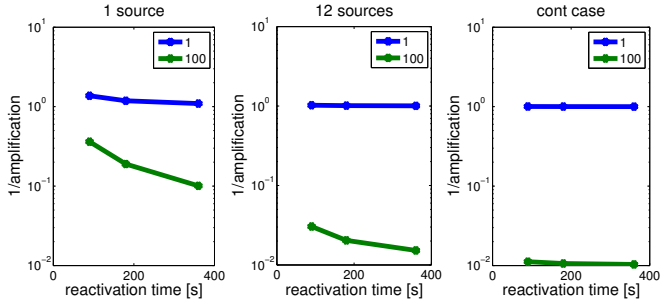

Figure 2: Test of the spatial effects: We used FEMLAB to test whether the spatiality in the system indeed effects the inhibition. The nucleus was modeled as a sphere with an influx of Cdc20 from different parts of the boundary. The inverse of the amplification of the "on-degradation" rate is plotted as a function of different maximal reactivation times. In the ODE case to which we compare the rate amplification is linear. We can thus compare the two cases and see how much the spatial case deviates from the non-spatial one. A pronounced difference was seen in the case where we limit the influx to a single point-like source (left most panel), this effect is much less pronounced when we let the influx come from 12 symmetrically spreaded point-like sources whose fraction of the nuclear area approximately equals that of the real cells [2] (middle panel). In the case of a contimous influx the spatial effect practically vanishes (right panel). Blue lines represent a case where the checkpoint doesn't amplify the degradation and the greeen lines a case where the amplification is 100 times. This plot is for the degradation model, similar results was obtained using the sequestering model (not shown).

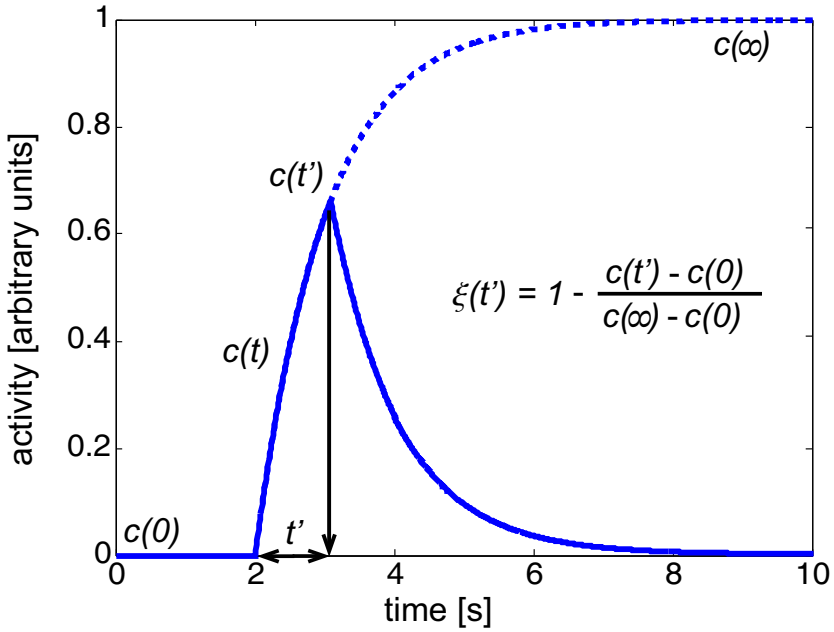

Figure 3: Definition of noise resistance: We note that $\xi \in [0,1]$ and that the higher value the better resistance. See the text for more details

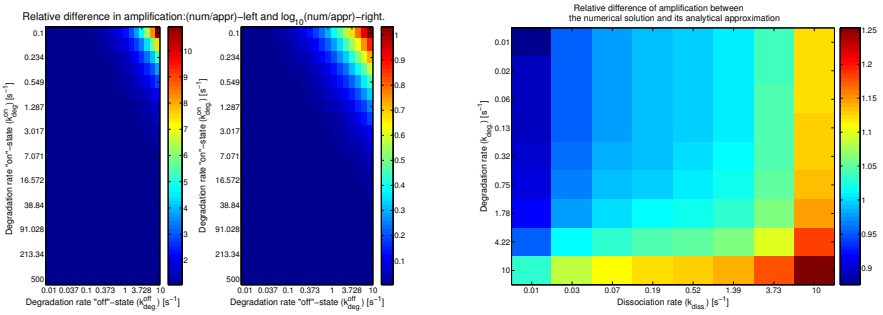

(a) Degradation model:ρ

(b) Sequestering model: ρ

Figure 4: **Degradation**: A comparison between the numerical and analytical solutions for the amplification in the degradation model, the estimate is very good as long as the checkpoint induced degradation $k^{on}_{deg.}$ is larger then the "natural"degradation $k^{off}_{deg.}$. Parameters used: $m_{tot} = 10$, $k_{prod.} = .1Ms^{-1}$, $k_{-m} = 100s^{-1}$ and $k_m = 1s^{-1}$. **Sequestering**: A comparison between the numerical and analytical solutions for the amplification in the sequestering model, we note that the approximation is good in the area of interest,(see section 4, eq53). Parameters used: $m_{tot} = 10$, $k_{prod.} = .01Ms^{-1}$, $k_{ass.} = 7.5s^{-1}$, $k_{-m} = 100s^{-1}$ and $k_m = 1s^{-1}$.

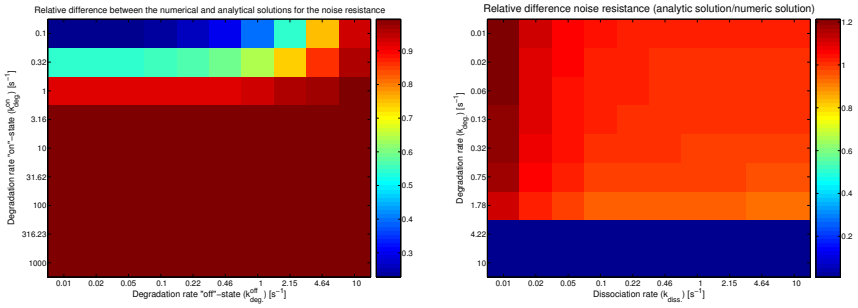

(a) Degradation model:ξ (b) Sequestering model: ξ

Figure 5: **Degradation**: A comparison between the numerical and analytical solutions for the noise resistance in the degradation model, the estimate is very good as long as the checkpoint induced degradation $k^{on}_{deg.}$ is larger then the "natural"degradation $k^{off}_{deg.}$. Parameters used: $m_{tot} = 10$, $k_{prod.} = .1Ms^{-1}$, $k_{-m} = 100s^{-1}$ and $k_m = 1s^{-1}$. **Sequestering**: A comparison between the numerical and analytical solutions for the noise resistance in the sequestering model. The reason the two last rows are all identically zero is that both the analytical and numerical solutions give the answer 0 and 0/0 isn't defined. Parameters used: $m_{tot} = 10$, $k_{prod.} = .01Ms^{-1}$, $k_{ass.} = 7.5s^{-1}$, $k_{-m} = 100s^{-1}$ and $k_m = 1s^{-1}$, the pulse length was $20s$ (first column) and $10s$ (all other columns).

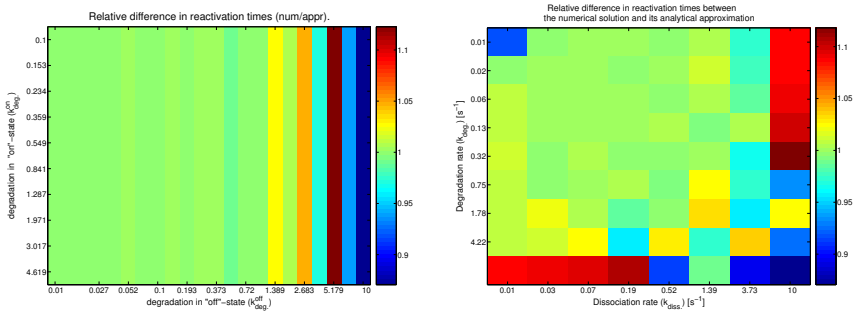

(a) Degradation model:τ (b) Sequestering model: τ

Figure 6: **Degradation**: A comparison between the numerical and analytical solutions for the reactivation time in the degradation model, note that the reactivation is independent of $k^{on}_{deg.}$. Parameters used: $m_{tot} = 10$, $k_{prod.} = .1Ms^{-1}$, $k_{-m} = 100s^{-1}$ and $k_m = 1s^{-1}$. **Sequestering**: A comparison between the numerical and analytical solutions for the reactivation time in the sequestering model, we note that the approximation is good in the area of interest, see section 4 (eq53). Parameters used: $m_{tot} = 10$, $k_{prod.} = .01Ms^{-1}$, $k_{ass.} = 7.5s^{-1}$, $k_{-m} = 100s^{-1}$ and $k_m = 1s^{-1}$.

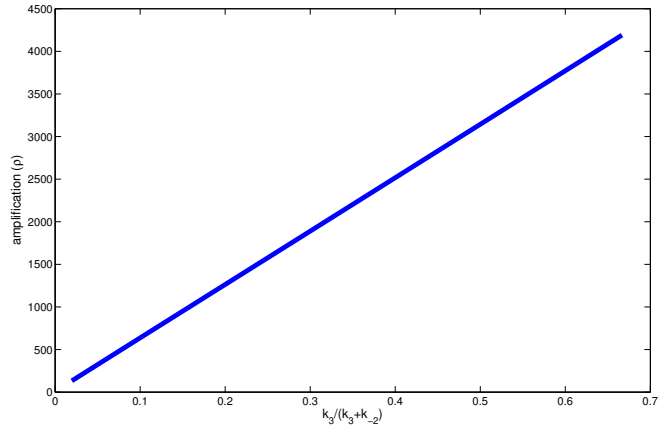

Figure 7: The relationship between the inhibition and the enhanced degradation rate "k_3"

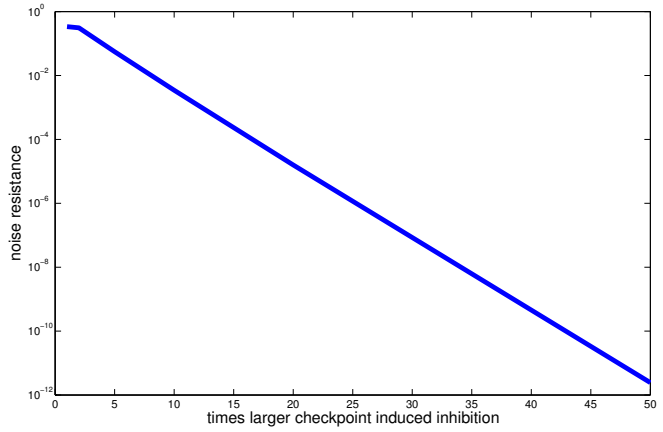

Figure 8: The decrease of the noise resistance as a function of the increase in checkpoint mediated inhibition

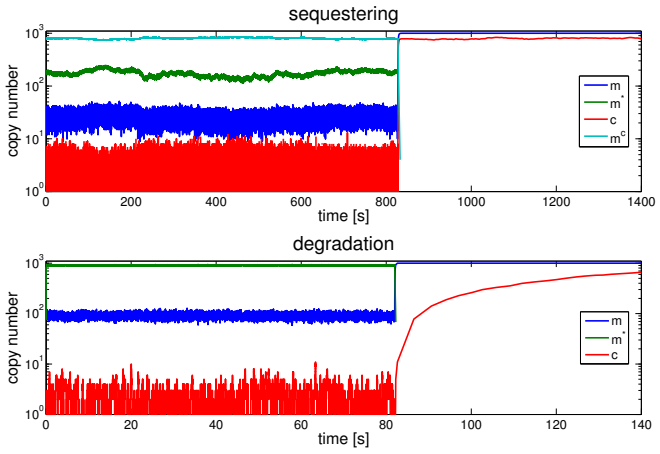

Figure 9: **Upper panel** :Gillespie simulation of the sequestering based system using with $9.375 * 10^6$ reactions. The analytical average of c (2.16) corresponds well with the numerical value (2.29) giving a 6 $\sim$ % error. The c-variance is ~ 2.3. The measured reactivation time was $\sim 2.12s$ compared with the analytical estimation of $2.28s$ ($\sim 7\%$ error). The numerical noise resistance was $\sim 100s$ and the analytical $99s$ ($\sim 1\%$ error). Parameters used: $m_{tot} = 1000$, $k_{prod.} = 8Ms^{-1}$, $k_{ass.} = 2(Ms)^{-1}$, $k_{-m} = 100s^{-1}$ and $k_m = 10s^{-1}$ $k_{diss} = 1s^{-1}$ and $k_{deg} = 0.01s^{-1}$. **Lower panel** :Gillespie simulation of the degradation based system using with $1.875 * 10^6$ reactions. The analytical average of c (2.197) corresponds well with the numerical value (2.20) giving a $< 1\%$ error. The c-variance is ~ 2.2. The measured reactivation time was $\sim 100s$ compared with the analytical estimation of $\sim 115s$ ($\sim 15\%$ error) . The numerical noise resistance was $\sim 0.08s$ and the analytical $\sim 0.11s$ ($\sim 30\%$error). Parameters used: $m_{tot} = 1000$, $k_{prod.} = 20Ms^{-1}$, $k_{on} = 0.01(Ms)^{-1}$, $k_{-m} = 100s^{-1}$ and $k_m = 10s^{-1}$ $k_{off} = 0.02s^{-1}$.

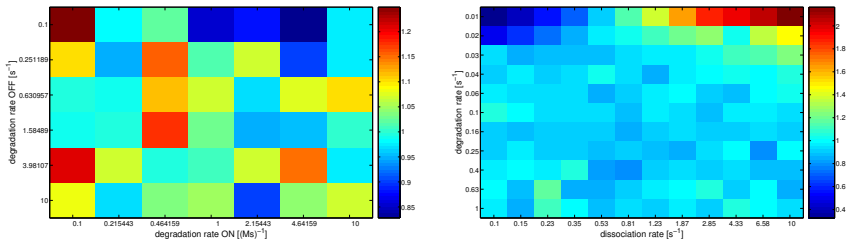

(a) degradation ρ

(b) sequestering ρ

(c) degradation τ

(d) sequestering τ

Figure 10: The amplification and reactivation for the two models. We here compare the analytical estimates with the stochatic numerical solutions from the gillespie algorithm. We note that the estimates get worse when we have, too much c, too little c and very fast reactivation. Parameters used:"degr.ρ": $100X20000$ iterations, $k_{prod} = 200s^{-1}$, $k_{-m} = 1000s^{-1}$ and $k_m = 100s^{-1}$. "degr.τ": $100X100000$ iterations, $k_{prod} = 20s^{-1}$, $k_{-m} = 100s^{-1}$ and $k_m = 1s^{-1}$. "seq.ρ": $10X150000$ iterations, $k_{prod} = 20s^{-1}$, $k_{ass.} = 20(Ms)^{-1}$, $k_{-m} = 100s^{-1}$ and $k_m = 10s^{-1}$. "seq.τ": $40X50000$ iterations, $k_{prod} = 20s^{-1}$, $k_{ass.} = 20(Ms)^{-1}$, $k_{-m} = 100s^{-1}$ and $k_m = 10s^{-1}$. all models $m_{tot} = 1000$.

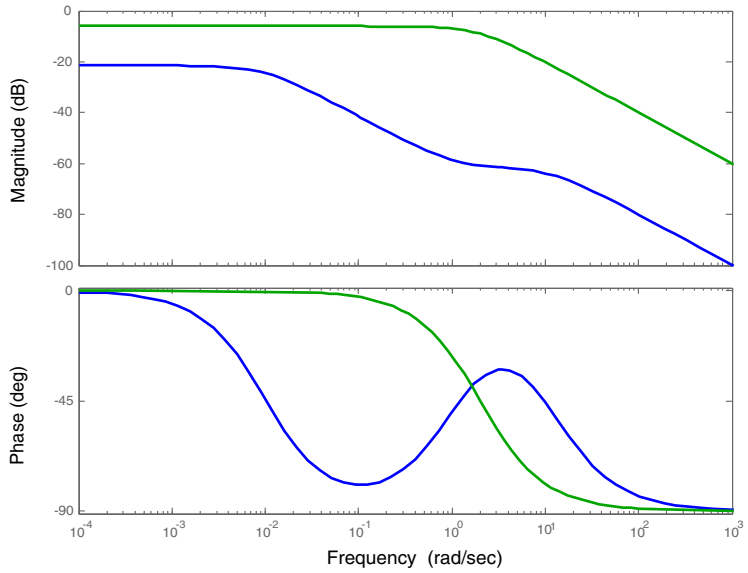

Figure 11: Bode plot and step response of the two different models. Sequestering model in blue and degradation in green.We see that both models damp high freqiencies whereas the sequestering model damps low and middle frequencies more efficiently. Parameters used: same as in figure 2A in the main text.